Indian Journal of Marine Sciences
Vol. 22, September 1993, pp. 188-193

Satellite altimetric detection of Somali eddies by signal processing technique

Sujit Basu, R M Gairola, A K Varma, N Gautam & P C Pandey
Meteorology and Oceanography Division, Space Applications Centre, Ahmedabad 380 053, Gujarat, India

Received 25 August 1992, revised 18 May 1993

Signal processing technique for detecting oceanic mesoscale eddies using dynamic topography data derived by satellite altimeters is described. This technique can be applied to single tracks of a satellite altimeter and consists of 3 steps. Firstly, the data time series is treated as an autoregressive sequence of finite order. The order best supported by the data, and the related autoregressive parameters are found by the modified covariance technique coupled with Cholesky decomposition. An analytical noise power spectral density which is used in the second step, in conjunction with a generic height signature due to an anticyclonic eddy, to design a matched filter is obtained by this method. Finally, the data are processed by the filter and the output is compared with a predetermined threshold to detect the presence (or, absence) of an eddy signature. This technique has been used to process several Geosat tracks near the Somali coast region of the Arabian Sea during the monsoon months of 1988. A few examples presented in the paper show that the technique is able to detect the great whirl, the southern gyre, the Socotra eddy and a few others. This approach alongwith sea surface temperature measurements by satellite radiometers can be a powerful tool for detecting oceanic mesoscale features.

Satellite altimeters, with their global coverage of world's oceans can play a significant role in detecting the mesoscale eddies. From the height of the satellite above a reference ellipsoid, one can accurately estimate the height of sea surface with respect to the reference ellipsoid. This, of course, requires several corrections for atmospheric refraction, instrument bias, etc. Further, if a precise marine geoid is known, one can also estimate the dynamic topography of the sea surface relative to marine geoid. This dynamic topography owes its origin to the oceanic flow and hence contains characteristic signatures of mesoscale features of oceanic movement like eddies and gyres. The dynamic topography data measured by altimeter onboard US Navy's satellite Geosat have been used in the present study to detect the presence of characteristic elevation signature due to a warm-core anticyclonic eddy in the Somali coast region of the Arabian Sea during monsoon months (July-Sept.) of 1988. The technique used here is according to the signal processing literature[1]. This technique has earlier been used for detecting Gulf stream eddies[2] and also for detecting seamounts[2-5] (the role of the signal being played by the characteristic geoidal undulation signature in the latter case).

Methods

Signal processing technique adopted presently processes single tracks of dynamic topography data derived by Geosat altimeter. Because of the presence of various errors like orbit error, residual error due to atmospheric and oceanic effects, uncertainty in the knowledge of the marine geoid etc., the data are quite noisy. The task therefore is to extract the typical sea surface height signature due to a mesoscale eddy from this noisy data set. This is accomplished by applying the matched filter algorithm followed by a threshold detector. The signal processing approach based on matched filter algorithm is elegantly documented[1-5]. The approach consists of the following 3 steps:

(i) The data series $z(t)$, $t=1, ..., n$ is treated as an autoregressive sequence of a finite order p in the following manner:

$$z(t)=\sum_{k=1}^{p} C_k z(t-k)+ W_p(t), \qquad t=p+1, ..., n \qquad ...(1)$$

where $W_p(t)$ is zero mean white noise of variance $\sigma^2(p)$ and $C_1, ..., C_p$ are the autoregressive coefficients. The standard autoregressive (AR) problem is next solved. This is to estimate the order p best supported by the data and the AR parameters

$\{C_k\}$ and $\sigma^2(p)$, given the data $\{z(t)\}$ and the maximum order p_{max}. The problem is solved by the modified covariance approach[6], wherein one minimizes (for each order $p=0, 1, 2, ..., p_{max}$) the average of the estimated forward and backward prediction error powers

$$\sigma^2(p)=\frac{1}{2}(\rho^f+\rho^b) \quad \ldots (2a)$$

$$\rho^f=\frac{1}{(n-p_{max})}\sum_{j=p_{max}+1}^{n}\left[Z(j)-\sum_{k=1}^{p}C_k Z(j-k)\right]^2 \quad \ldots (2b)$$

$$\rho^b=\frac{1}{(n-p_{max})}\sum_{j=1}^{n-p_{max}}\left[Z(j)-\sum_{k=1}^{p}C_k Z(j+k)\right]^2 \quad \ldots (2c)$$

where $p=0,1,2,...,p_{max}$.

Minimization is done with respect to the coefficients $\{C_k\}$ and the resulting equations are solved by Cholesky decomposition technique[6]. After substituting for the estimated coefficients, Eqs (2a-2c) give the estimate of the white-noise variance. This estimate is then used to compute the Akaike information criterion[7] (AIC) for each p

$$\mathrm{AIC}(p)=n\ln[\sigma^2(p)]+2p \quad \ldots (3)$$

The particular p that minimizes AIC(p) is identified; the corresponding AR parameters then define the particular AR model which is best supported by the available data. The power spectral density (PSD) of the underlying noise process $N(t)$ can then be computed analytically[2]. This approach of PSD estimation is very modern and is far superior to the classical approach like periodogram etc.[8]

(ii) This step involves the designing of the matched filter, which is an algorithm, optimum in terms of detecting a given signal in noisy data[4,5]. Once the signal and the noise PSD are known, the transfer function of the filter can be written as

$$H'(f)=\frac{M'(-f)}{S(f)} \quad \ldots (4)$$

where $M'(f)$ is the signal Fourier transform and $S(f)$ is the PSD estimated in step (i). In the present case, role of signal is played by a generic signature due to a warm-core anticyclonic eddy. Following earlier reports[2] this signature was modelled as

$$m(x)=D\exp[-9.21\,(x/W)^2] \quad \ldots (5)$$

where x = distance along satellite ground track, D = maximum signature height and W = signature width. Conversion from spatial to temporal domain and *vice versa* is easily accomplished by means of the velocity of the sub-satellite point which is 6.8 km. sec^{-1} for Geosat. The impulse response of the matched filter is obtained by the inverse Fourier transform. Processing the data series $\{z(t)\}$ with this matched filter amounts to taking the convolution

$$y(t)=\sum_{k=-\infty}^{+\infty}h(k)z(t-k) \quad \ldots (6)$$

where $h(k)$ denotes the impulse response of the filter. Because of the finite support property of signal and the filter impulse response there will be only a finite number of non-zero terms in this convolution. The output of the filter is conveniently scaled by the rms signal-to-noise ratio (SNR) i.e.

$$Y(t)=\text{scaled output}=y(t)/\mathrm{SNR} \quad \ldots (7)$$

$$\text{where} \qquad \mathrm{SNR}=\sqrt{\sum_{k=-\infty}^{+\infty}h(k)m(-k)} \quad \ldots (8)$$

This scaling ensures that the output contains a random component having standard deviation of unity.

(iii) The final step consists of applying a threshold detector. The output $Y(t)$ is compared with a predetermined threshold (TH), chosen to produce a specified average false alarm rate (FAR)

$$\mathrm{TH}=[2\ln(F_m/\mathrm{FAR})]^{1/2} \quad \ldots (9)$$

In Eq. (9) F_m is the rms bandwidth of the filter output

$$F_m=(2\pi)^{-1}\cos^{-1}(X/\mathrm{SNR}^2) \quad \ldots (10)$$

$$X=\sum_{k=-\infty}^{+\infty}h(k)m(1-k) \quad \ldots (11)$$

The maximum-likelihood estimate of the location of detected eddy signature is the value of t for which $Y(t)$ achieves a local maximum above the threshold TH. One can also estimate the detected amplitude of the signature which is

$$A=DY(t_0)/\mathrm{SNR} \quad \ldots (12)$$

where $Y(t_0)$ denotes the scaled output at the detection location t_0. This completes the presentation of the signal processing technique adopted here. The sea surface height data obtained by the altimeter onboard the US Navy's satellite Geosat at 13.5 GHz with a nominal data rate of 1 Hz,

has been used in this study. The Geosat was launched in 1985, primarily for geodetic mission. However, the satellite was manouvered into the exact repeat mission (ERM) orbits on 8 Nov. 1986 primarily for computing sea level variability and other oceanographic missions. The data was first corrected for atmospheric and oceanographic effects and many pairs of Geosat tracks were selected for eddy detection purpose using the signal processing technique. Data were extracted near the Somali coast region during the monsoon months of 1988.

Results and Discussion

The approach sketched above was applied to numerous Geosat tracks passing over the region of study from 5°S to 15°N and 40° E to 65°E during July to September 1988. The data consisted of the dynamic topography, corrected for various atmospheric and oceanographic effects. Some of the tracks were collinear. Bruce[9] monitored the time series of temperature sections obtained along the tanker sea lanes across the Somali Basin for 4 consecutive years (1975-1978). Evidence suggested that the great whirl first forms between 4°N to 12°N during late May and tends to remain approximately in this location throughout the entire southwest monsoon.

An eddy of smaller horizontal dimensions which appears to be associated with the great whirl was also found each year off Socotra between 12° and 15° N. Also during some years an eddy was observed south of about 5° N (southern gyre) and adjacent to the southern boundary of the great whirl and to the eastern African coast. A comprehensive summary of the observations of currents and temperature in the Somali current regime has further been provided by Schott[10], which shows that a two gyre system forms in most of the years with the onset of the monsoon and remains approximately stationary with slow northward migration until mid August. Thus the detection of an eddy at about the same location in 2 or more collinear tracks (with a repeat period of about 17.03 days) shows the success of the technique. Few examples of processing Geosat tracks are presented as below.

The first example involves a descending Geosat pass on 17th August from (15°49'12" N, 53°54'36" E) to (4°55' S, 45°31'48" E) marked as 1 in Fig. 1. and Fig. 2B depicts the corrected sea surface height (dynamic topography measured relative to a marine geoid) along this track. Upper panel of the same figure shows the scaled output from the matched filter. The horizontal dashed line in this and subsequent figures indicates the detection threshold corresponding to a chosen false alarm rate (FAR) of 0.1 alarms/megameter.

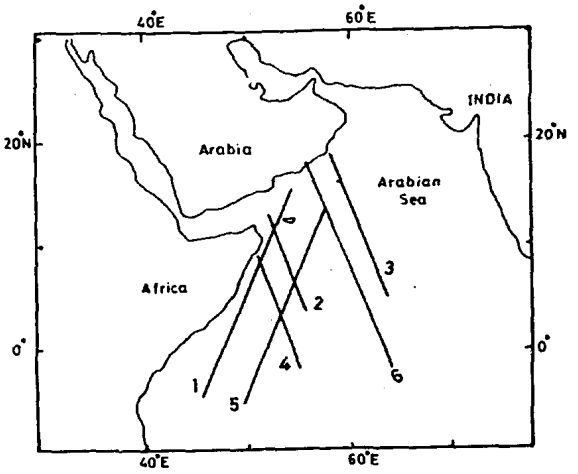

Fig. 1—The region of study in the Arabian Sea with selected Geosat tracks superimposed

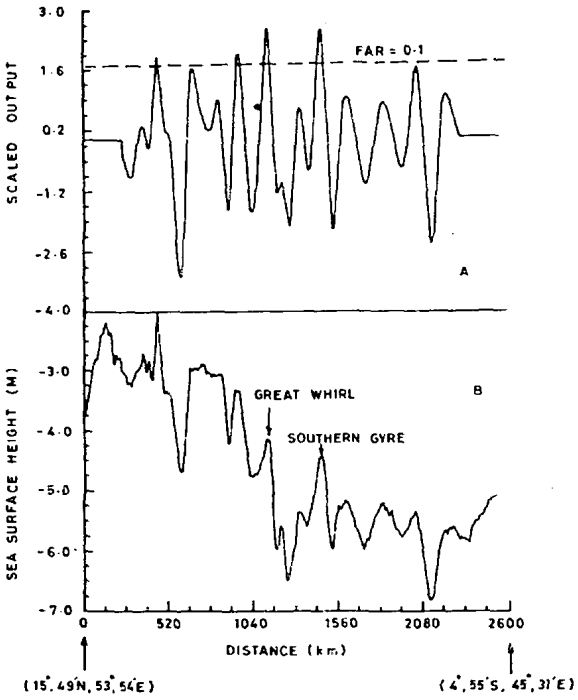

Fig. 2—The results of processing track no. 1. (A) Geosat altimeter data, (B) The matched filter output, with detection threshold indicated by dashed line. The corresponding false alarm rate (FAR) in this and subsequent figures is measured in alarms/megameter. (Note the truncation of the output at its ends to avoid edge effects due to numerical convolution)

This value has been used earlier[2] for detecting Gulf stream eddies and is found to be suitable here. It is also to be noted that the filter output has been truncated at the ends so as to avoid edge effects arising out of numerical convolution. The number of points to be deleted at both the ends vary from case to case and is decided by the algorithm itself. The output shows two detections at (6°37'12" N, 50°7'48" E) and at (3°56'24" N, 49°3'36" E). The first one is interpreted as the signature of the great whirl mentioned earlier and the second one is interpreted as the signature of a section of the southern gyre since these locations seem to agree with earlier observational studies and also with results of model simulations[11,12]. Maximum-likelihood estimates of the amplitudes of both the signatures are 1.37 m. It is to be noted that there are 2 other threshold crossings in the filter output; one being at (8°4'12" N, 50°42'36" E). This may be again a cross-section of the great whirl, since generally this is formed between 5°N and 9°N. However, another peak at (12°9' N, 52°22'12" E) is probably due to a data error caused by the presence of a small island Abd al-Kuri. Figure 3 depicting a repeat-track on 3rd September shows that great whirl is again detected at the same location (just above the detection threshold in Fig. 3). However, the southern gyre signature is no more detected. This may, of course, signify the vanishing of the southern gyre in September or at least its weakening (so that the corresponding height signature is below the limit of detectability). The detection of great whirl in both the tracks is not surprising since it is known to be persistent during the monsoon months.

The second example concerns the processing of an ascending Geosat track on 19th August (marked as 2 in Fig. 1). This is a relatively short track, < 1000 km in extent. In Fig. 4 a detection is seen at (6°21'36" N, 54°32'24" E). Again this is interpreted as the signature of the great whirl. This location is quite different from that in the previous example. There is, however, no contradiction here since the horizontal extent of the great whirl is known to be of the order of 400-600 km.

The third example involves a descending pass on 20th August. As shown in Fig. 5 two signatures are detected in this track, one at (14°48'36" N, 59°55'48" E) and the other at (15°58'48" N, 59°25'48" E). Both are very prominent, with maximum-likelihood estimates of signature amplitudes of 2.37 and 2.49 m respectively.

The fourth example illustrates a track on 19th August passing from (2° S, 54°55'12" E) to

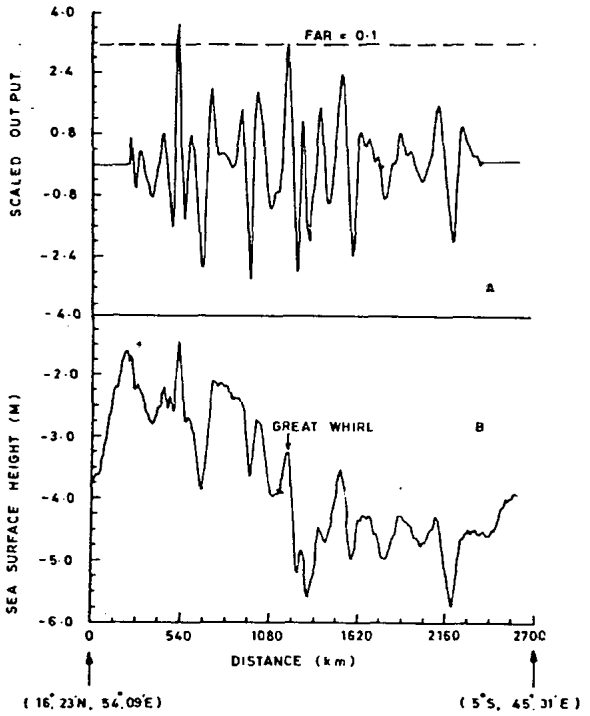

Fig. 3—The results of processing a track, which is a repeat of track no. 1. (A) Geosat altimeter data, (B) The matched filter output

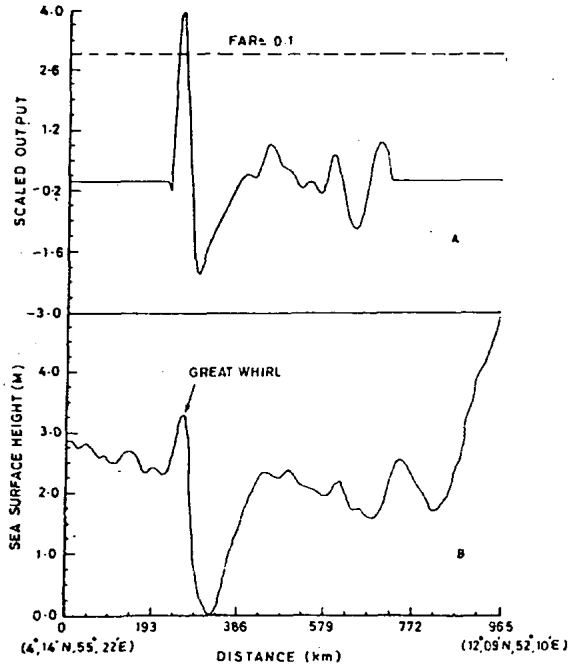

Fig. 4—Example of eddy detection in an ascending Geosat track on 19th August 1988 (The detection is interpreted as a section of the great whirl)

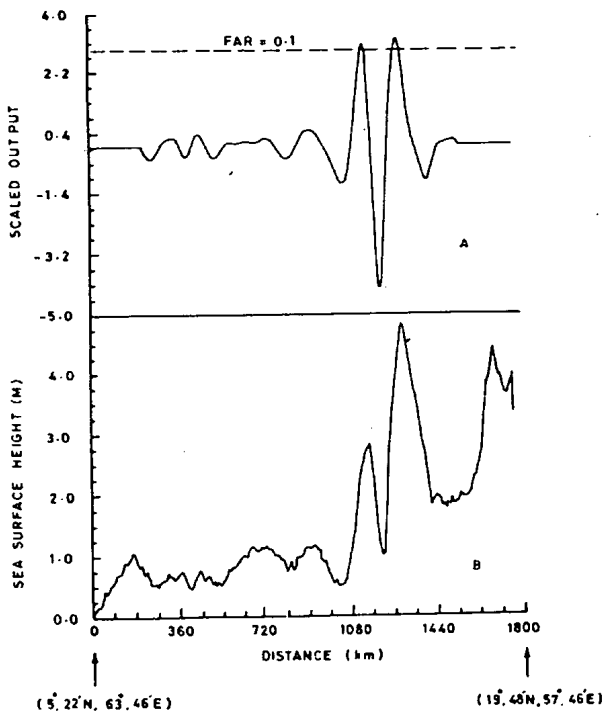

Fig. 5—Example of eddy detection in an ascending Geosat track on 20th August (The track marked 3, as in Fig. 1)

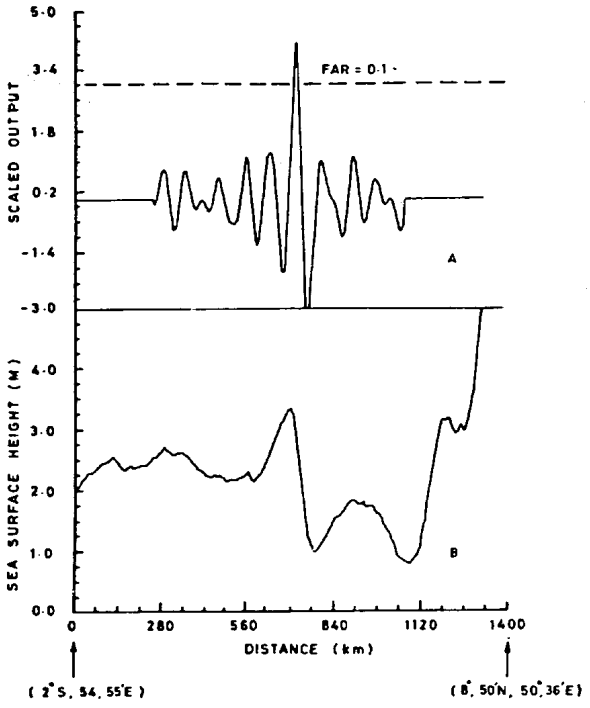

Fig. 6—Detection of the southern gyre in an ascending Geosat track on 19th August

(8°50'24" N, 50°36'24" E). Figure 6 shows the matched filter detection of an eddy signature at (3°52'12" N, 52°35'24" E). This is again to be interpreted as the detection of southern gyre as in the first example. The fifth example in Fig. 7 is again a detection of the great whirl at (6°3'36" N, 54°20'24" E).

The final example involves an ascending Geosat pass on 11th July. The track extends from (2°29'24" S, 63°57' E) to (17°46'12" N, 55°42'36" E) and is marked as 6 in Fig. 1. The filter output shows a threshold crossing at about (12°35'24" N, 57°53'24" E) which is at the northeast of Socotra island (Fig. 8). Accordingly, this is interpreted as the detection of the Socotra eddy. This signature was also detected at about the same location in collinear tracks on 28th July and 31st August. It is also to be noted that model studies also show prominent eddy in this region during southwest monsoon. Ali[13] had found the evidence of an eddy in this region using thermal data of INSAT 1-B very high resolution radiometer (VHRR) during June 1985.

One can see from the figures presented (Figs 2-8) that almost all the height signatures detected by the signal processing technique are very prominent. One might be tempted to infer that they

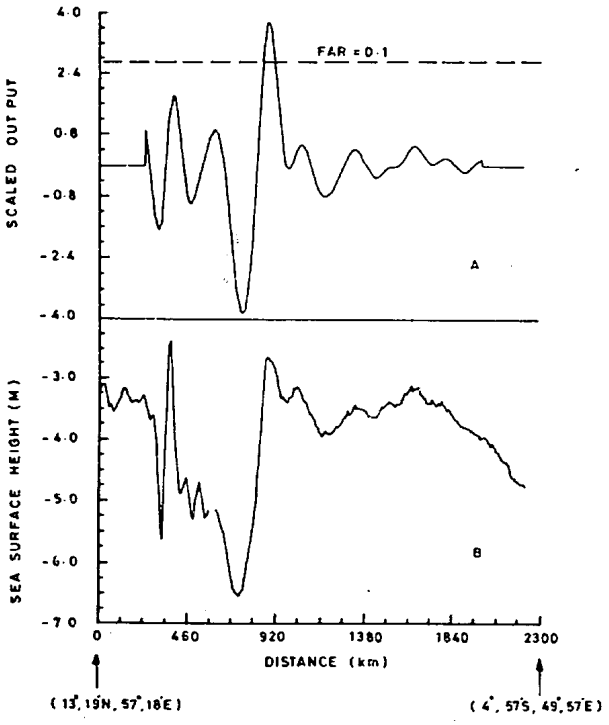

Fig. 7—The results of processing track no. 5. The great whirl is again detected

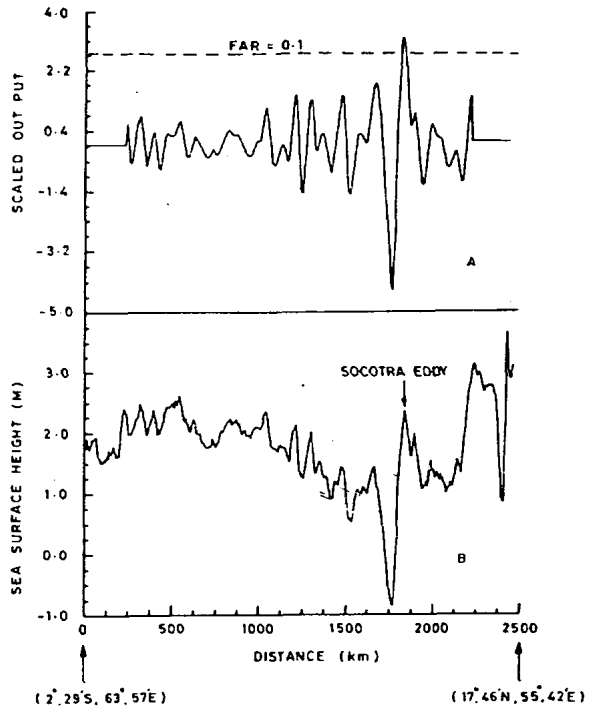

Fig. 8—Detection of the Socotra eddy in an ascending Geosat track on 11th July. (This was also detected in the collinear tracks on 28th July and 31st August)

could be detected visually, simply by looking at the corresponding sea surface height curves without bothering to apply the lengthy signal processing technique. The signatures are prominent because the corresponding eddies themselves are very prominent. However, the aim of this study was mainly to demonstrate the power of the technique which is equally suitable for detecting eddies with smaller dimensions escaping detection by visual inspection. Also, simple visual survey is subjective and almost impossible to apply for huge data sets expected to be available from recently launched ERS-1 and Topex/Poseidon. These satellites are expected to provide dynamic topography data with much better precision than Geosat. This is primarily because of the improved estimates of geoid and more accurate orbit error removal. Further in the case of ERS-1, water vapour correction is much more accurate because of the presence of onboard microwave radiometer. It is thus expected that the dynamic topography data from these satellites, as and when they become available to the oceanographic community, will provide a much better input for the signal processing technique described in this paper.

Acknowledgement

Authors are indebted to Dr. J V White, The Analytic Sciences Corporation, 55 Walkers Brook Drive, Reading, MA 01867, USA, for his valuable suggestions and comments.

References

1 Helstrom C V, *Statistical theory of signal detection*, (Pergamon, Oxford) 1968, pp. 467.
2 Brammer R F, Pass R P & White J V, *IEEE Trans Automat Control*, AC-28 (1983) 363.
3 White J V, Sailor R V, Lazarewicz A R & LeSchak A R, *J Geophys Res*, 88 (1983) 1541.
4 Basu S, Gairola R M & Pandey P C, *Mar Geod*, 14 (1990) 121.
5 Gairola R M, Basu S & Pandey P C, *Int J Rem Sensing*, 13 (1992) 971.
6 Kay S M, *Modern spectrum analysis: theory and application*, (Prentice Hall, New Jersey) 1988, pp. 543.
7 Akaike H, *IEEE Trans Automat Control*, AC-19 (1974) 716.
8 Gangopadhyay A, Cornillon P & Jackson L B, *J Geophys Res*, 94 (1989) 16215.
9 Bruce J G, *J Geophys Res*, 84 (1979) 7742.
10 Schott F, *Prog Oceanogr*, 12 (1983) 357.
11 Luther M E & O'Brien J J, *Prog Oceanogr*, 14 (1985) 353.
12 Luther M E & O'Brien J J, in *Coupled ocean-atmosphere models*, edited by J C J Nihoul, (Elsevier, Amsterdam) 1985, 405.
13 Ali M M, *Int J Rem Sensing*, 11 (1990) 41.